On the Stability Properties of Extremum Seeking Dynamics Under Persistent Gradient Jamming: A Switching Systems Approach

Felipe Galarza-Jimenez, Jorge I. Poveda, Gianluca Bianchin, Emiliano Dall'Anese

Abstract— **The adoption of automated, self-tuning, and networked control technologies in cyber-physical and engineering systems may come at the cost of an increased vulnerability to adversarial attacks in the form of jamming signals. While a persistent attack in a feedback controller may be difficult to continuously identify or mitigate, for a broad class of closed-loop systems it suffices to achieve mitigation "sufficiently often" in order to preserve the stability properties. In this paper, we explore for the first time the resilience properties of extremum seeking (ES) controllers with respect to a class of jamming signals that are purposely designed to destabilize optimization-based controllers: *persistent jamming of gradient directions*. By leveraging Lyapunov-based arguments for switched systems and singular-perturbation theory for hybrid dynamical systems, we characterize families of jamming signals under which gradient-based ES, Newton-like ES, and Hybrid Accelerated ES controllers can provably preserve stability.**

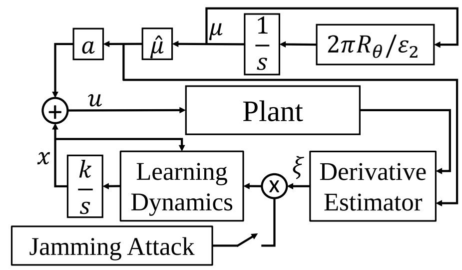

Fig. 1: Scheme of ESC under gradient jamming.

I. INTRODUCTION

Automation and self-tuning technologies are becoming ubiquitous in many modern engineering systems. Increased levels of autonomy often come at the cost of vulnerabilities to malicious entities aiming to destabilize the system via cyber or physical attacks [1]–[3]. Controllers synthesized according to principled first-order optimization methods in model-predictive control (MPC) [4], autonomous optimization [5], [6], and extremum seeking control [7], [8] appear to be particularly vulnerable to jamming signals that corrupt the gradient information. From an adversarial standpoint, these attacks are attractive because they can be executed by simply modifying *one bit* in the controller [2]. Indeed, in engineering systems and, e.g., chemical processes and bio-reactors endowed with real-time optimization algorithms and optimization-based controllers, persistent jamming can easily induce instability [9]. Nevertheless, to the best of our knowledge, control theoretic tools to study the effects of attacks on these algorithms, and the design of controllers that securely steer the system towards the optimal operating point, are still lacking [10].

In this paper, we study for the first time the robustness of averaging-based extremum seeking (ES) dynamics under gradient jamming by using tools from control theory and hybrid dynamical systems (HDS). The main idea is illustrated in Fig. 1, where we show a typical ES feedback controller, comprised of a plant, a derivative estimator, and a learning algorithm, which is subject to gradient jamming by a persistent inversion of the sign of the signal ξ. In this case, while it may not be possible (or not feasible from an economic point of view, see [2]) to guarantee that the jammed signal is always corrected or protected *a priori* for all times $t \geq 0$, stability of the closed-loop system could still be guaranteed provided the time incidence of the attacks is "sufficiently" mitigated, e.g., if there exists $T > 0$ such that the attacks are mitigated during, at least, a certain percentage of time $p \in (0, 1)$ of the interval $[t, t+T]$, for all $t \geq 0$. Such type of mitigation strategies have been studied in the cyber-security literature [2], [3], but they have not been explored and formalized in complex controllers with multiple time scales such as ES.

With this motivation, in this paper we present the first general analysis of averaging-based ES dynamics under persistent gradient jamming. In particular, we consider attacks, modeled by a switching signal $q : \mathbb{R}_{\geq 0} \to \{-1, 1\}$ that persistently changes the sign of the estimated gradient of the cost function used by the controller to regulate the input u. By using Lyapunov-based tools for HDS [11], [12], we provide sufficient conditions on q to guarantee that the closed-loop system under attacks retains the stability properties of the nominal system with no attacks. Such characterization of q is provided for three different types of ES dynamics: (a) Gradient descent-based ES [13], [14]; (b) Newton-like ES [15], [16]; and (c) Hybrid Accelerated ES [17]. Our results reveal the effect (or lack of effect) of the convexity and Lipschitz parameters of the response map on the bounds that characterize the "safe" attacks q that preserve the stability properties of the system. Our results also uncover new trade-offs between fast convergence and resilience to attacks in nominal and accelerated gradient-based ES algorithms. Moreover, we also present the first stability result for an ES controller that continuously switches between Gradient descent-based ES and Newton-Like ES (this result may be of independent interest). To the knowledge of the authors, the results of this paper are also the first that combine switched

The authors are with the Department of Electrical, Computer, and Energy Engineering, University of Colorado, Boulder, CO. Contact Email: {felipe.galarzajimenez@colorado.edu}.

systems theory and averaging/singular perturbation theory for the analysis of extremum seeking controllers.

The remainder of this paper is organized as follows. Section II presents some preliminaries regarding notation, hybrid dynamical systems, and stability notions. Section III presents our main results. Section IV presents the analysis and proofs of the theorems. Section V presents numerical examples, and finally Section VI concludes the paper.

II. PRELIMINARIES

Given a compact set $\mathcal{A} \subset \mathbb{R}^n$ and a vector $z \in \mathbb{R}^n$, we use $|z|_{\mathcal{A}} := \min_{s\in\mathcal{A}} \|z - s\|_2$ to denote the minimum distance of z to $\mathcal{A}$. We use $\mathbb{S}^1 := \{z \in \mathbb{R}^2 : z_1^2 + z_2^2 = 1\}$ to denote the unit circle in $\mathbb{R}^2$, and $\mathbb{T}^n := \mathbb{S}^1 \times \mathbb{S}^1 \times \ldots \times \mathbb{S}^1$ to denote the n^{th} Cartesian product of $\mathbb{S}^1$. Given vectors $p_1, p_2 \in \mathbb{R}^n$, we also use $(p_1, p_2) = (p_1^\top, p_2^\top)^\top$ to simplify notation. This paper deals with systems modeled as hybrid dynamical systems (HDS) [11] of the form

$$p \in C,\ \dot{p} \in F(p), \qquad p \in D,\ p^+ \in G(p), \tag{1}$$

where $p \in \mathbb{R}^n$ is the state, $F : \mathbb{R}^n \rightrightarrows \mathbb{R}^n$ is the flow map, $G : \mathbb{R}^n \rightrightarrows \mathbb{R}^n$ is the jump map, $C \subset \mathbb{R}^n$ is called the flow set, and D is called the jump set. The *data* of a HDS is described by $\mathcal{H} = \{C, F, D, G\}$. Solutions to systems of the form (1) are defined on hybrid time domains. Under mild assumptions on the data, this permits the use of graphical convergence notions to establish sequential compactness results for the solutions of (1) (e.g., the limit of a sequence of solutions is also a solution). A set $E \subset \mathbb{R}_{\geq 0} \times \mathbb{Z}_{\geq 0}$ is called a *compact* hybrid time domain if $E = \cup_{j=0}^{J-1}([t_j, t_{j+1}], j)$ for some finite sequence of times $0 = t_0 \leq t_1 \ldots \leq t_J$. The set E is a hybrid time domain if for all $(T, J) \in E$, $E \cap ([0, T] \times \{0, \ldots, J\})$ is a compact hybrid time domain.

Definition 1: A function $p : \text{dom}(p) \mapsto \mathbb{R}^n$ is a hybrid arc if $\text{dom}(p)$ is a hybrid time domain and $t \mapsto p(t, j)$ is locally absolutely continuous for each j such that the interval $I_j := \{t : (t, j) \in \text{dom}(p)\}$ has nonempty interior. A hybrid arc p is a *solution* to (1) if $p(0, 0) \in \overline{C} \cup D$, and the following two conditions hold:

1) For each $j \in \mathbb{Z}_{\geq 0}$ such that I_j has nonempty interior: $p(t, j) \in C$ for all $t \in \text{int}(I_j)$, and $\dot{p}(t, j) \in F(p(t, j))$ for almost all $t \in I_j$.
2) For each $(t, j) \in \text{dom}(p)$ such that $(t, j+1) \in \text{dom}(p)$: $p(t, j) \in D$, and $p(t, j+1) \in G(p(t, j))$. □

Definition 2: A hybrid solution p is said to be forward pre-complete if its domain is compact or unbounded, i.e., if the flows do not generate finite escape times. A hybrid solution is said to be forward complete if its domain is unbounded. A hybrid solution is maximal if there does not exist another solution ψ to $\mathcal{H}$ such that $\text{dom}(p)$ is a proper subset of $\text{dom}(\psi)$, and $p(t, j) = \psi(t, j)$ for all $(t, j) \in \text{dom}(p)$. □

Given a compact set $\mathcal{A} \subset C \cup D$, system (1) is said to render $\mathcal{A}$ uniformly globally asymptotically stable (UGAS) if there exists a class $\mathcal{KL}$ function [11, Def. 3.38] β such that every solution of (1) satisfies $|p(t, j)|_{\mathcal{A}} \leq \beta(|p(0, 0)|_{\mathcal{A}}, t+j)$ for all $(t, j) \in \text{dom}(p)$. We will also consider ε-perturbed or parameterized HDS of the form

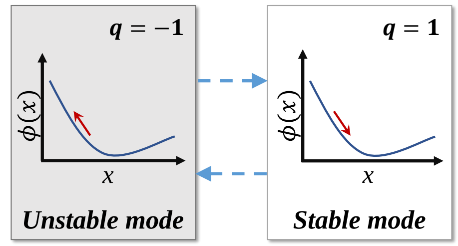

Fig. 2: The system switches between a stable mode ($q = 1$) and an unstable mode ($q = -1$).

$$p \in C,\ \ \dot{p} \in F_\varepsilon(p), \qquad p \in D,\ \ p^+ \in G(p). \tag{2}$$

where $\varepsilon > 0$. A compact set $\mathcal{A} \subset C$ is said to be Semi-Globally Practically Asymptotically Stable (SGPAS) as $\varepsilon \to 0^+$ for system (2), if there exists a class $\mathcal{KL}$ function β such that for every $\delta_0 > \nu > 0$ there exists $\varepsilon^* > 0$ such that for all $\varepsilon \in (0, \varepsilon^*)$ every solution of (2) with $|p(0, 0)|_{\mathcal{A}} \leq \delta_0$ satisfies $|p(t, j)|_{\mathcal{A}} \leq \beta(|p(0, 0)|_{\mathcal{A}}, t+j) + \nu,\ \forall\ (t, j) \in \text{dom}(p)$. The notion of SGPAS can be extended to systems that depend on multiple parameters $\varepsilon = [\varepsilon_1, \varepsilon_2, \ldots, \varepsilon_\ell]^\top$. In this case, and with some abuse of notation, we say that the system (2) renders the set $\mathcal{A}$ SGPAS as $(\varepsilon_\ell, \ldots, \varepsilon_2, \varepsilon_1) \to 0^+$, where the parameters are tuned *in order*, starting from ε_1, that is, ε_2 may depend on ε_1, and ε_3 may depend on ε_2, etc.

III. MODEL AND MAIN RESULTS

In this paper, we model the attack on the ES controllers as a switching signal $t \mapsto q(t)$ taking values in the set $Q := Q_s \cup Q_u$, where $Q_s = \{1\}$ describes the stable mode (no attack), and $Q_u := \{-1\}$ describes the unstable mode (jamming attack) as pictured in Fig. 2. We will impose two regularity conditions on q: (a) an *average dwell-time constraint* [18] that regulates how frequent the state q can switch its value; and (b) a *time-ratio constraint* [12], [19] on the activation time of the unstable mode. For a positive integer N_0 and a positive number η_1, the average dwell-time constraint has the form

$$N(s, t) \leq \eta_1(t - s) + N_0, \quad \forall \ \ 0 \leq s \leq t, \tag{3}$$

where $N(s, t)$ denotes the number of switches of q in the interval $[s, t]$. Similarly, for any $T_0 \in \mathbb{R}_{\geq 0}$ and $\eta_2 \in [0, 1)$, the time-ratio constraint has the form

$$T(s, t) \leq \eta_2(t - s) + T_0, \tag{4}$$

where $T(s, t)$ denotes the *total activation time* of the unstable mode Q_u during the the interval of time $[s, t]$, i.e., $T(s, t) = \int_s^t \mathbb{I}_{Q_u}(q(r))dr$, where $\mathbb{I}_{Q_u}(\cdot)$ is the indicator function for the set Q_u. In this way, time-ratio constraints with larger values of η_2 describe switching signals that are allowed to spend more time on the unstable modes compared to the stable modes. Similarly, average dwell-time constraints with large values of η_1 describe switching signals that are allowed to switch more frequently.

Given that the analysis of ES in dynamic plants relies on a time-scale separation between the dynamics of the plant and the dynamics of the controller, for the type of attacks considered in this paper it suffices to study the ES problem in static maps ϕ. This is the case because once a jammed ES controller is guaranteed to be stable for a static map that describes the steady-state input-to-output map of a plant, stability of the closed loop system with the actual dynamic plant in the loop will follow by using a standard singular perturbation argument, provided the plant is stable and the time-scale separation is sufficiently large [20, Thm. 2].

To make our analysis tractable, we will make the following standing assumption on the static maps.

Assumption 1: ϕ is $\mathcal{C}^2$, strongly convex, and its unique minimizer is $u^* \in \mathbb{R}^n$; further, $\nabla\phi$ is globally Lipschitz. □

A consequence of Assumption 1 is the existence of positive constants $\kappa, \ell > 0$ such that $\frac{\kappa}{2}|u-u^*|^2 \leq \phi(u)-\phi(u^*) \leq \frac{\ell}{2}|u-u^*|^2$, for all $u \in \mathbb{R}^n$. These constants will play an important (qualitative) role in the results presented shortly.

The ES problem can then be formalized as the following model-free optimization problem

$$\min_{u\in\mathbb{R}^n} \ \phi(u), \tag{5}$$

where only real-time evaluations of ϕ are available to the controller.

A. Hybrid Automaton with Monitoring States

Working with switching ES dynamics adds an extra layer of difficulty to the analysis of the system due to the time-varying nature of the switching signal q. To address this issue, we can use a (time-invariant) hybrid automaton that generates switching signals q that satisfy the constraints (3) and (4). Moreover, this automaton can also generate *any* signal satisfying these constraints provided the initial conditions of the system are appropriately selected. The following lemma, originally established in [12, Lemma 7], captures this idea.

Lemma 1: Consider a set-valued HDS with state $\vartheta := (\tau_1, \tau_2, q) \in \mathbb{R}_{\geq 0} \times \mathbb{R}_{\geq 0} \times Q$, and dynamics given by

$$\vartheta \in C_M := [0, N_0] \times [0, T_0] \times Q, \tag{6a}$$

$$\begin{pmatrix} \dot{\tau}_1 \\ \dot{\tau}_2 \\ \dot{q} \end{pmatrix} \in F_M(\vartheta) := \begin{pmatrix} [0, \eta_1] \\ [0, \eta_2] - \mathbb{I}_{Q_u}(q) \\ 0 \end{pmatrix}, \tag{6b}$$

$$\vartheta \in D_M := [1, N_0] \times [0, T_0] \times Q, \tag{6c}$$

$$\begin{pmatrix} \tau_1^+ \\ \tau_2^+ \\ q^+ \end{pmatrix} \in G_M(\vartheta) := \begin{pmatrix} \tau_1 - 1 \\ \tau_2 \\ Q\backslash\{q\} \end{pmatrix}, \tag{6d}$$

where $\mathbb{I}_{Q_u}(\cdot)$ is the indicator function for the set Q_u, $T_0 \geq 0$, $N_0 \in \mathbb{Z}_{\geq 1}$, $\eta_1 > 0$, and $\eta_2 \in (0, 1)$. Then, for every solution ϑ of (6) corresponds a hybrid time domain that satisfies conditions (3) and (4). Moreover, each switching signal q and hybrid time domain satisfying conditions (3) and (4) can be generated by (6). □

With Lemma 1 at hand, we can study the stability properties of the ES dynamics under persistent jamming by studying the stability properties of the interconnection between the ES dynamics and the HDS (6).

B. Extremum Seeking Dynamics with Gradient Jamming

The nominal ES algorithms that we consider in this paper are conceptually similar to those studied in [13], [14], [21], and [15]. In particular, the algorithms implement periodic excitation signals that facilitate the extraction in real-time of the gradient and/or Hessian information of ϕ. This dither signals can be generated by an oscillator of the form

$$\varepsilon_2\dot{\mu} = 2\pi\mathcal{R}_\theta\mu, \quad \mu \in \mathbb{T}^n, \quad \varepsilon_2 > 0, \tag{7}$$

where the matrix $\mathcal{R}_\theta \in \mathbb{R}^{2n\times 2n}$ is block diagonal with i^{th} block given by $\mathcal{R}_{\theta_i} := \begin{bmatrix} 0 & \theta_i \\ -\theta_i & 0 \end{bmatrix}$, and $\theta_i > 0$. In particular, the odd components of the solutions of (7) are

$$\mu_i(t) = \mu_i(0)\cos\left(\frac{2\pi}{\varepsilon_2}\theta_i t\right) + \mu_{i+1}(0)\sin\left(\frac{2\pi}{\varepsilon_2}\theta_i t\right), \tag{8}$$

for all $i \in \{1, 3, 5, \ldots, 2n-1\}$, where $\mu_i(0)^2+\mu_{i+1}(0)^2 = 1$. We use $\hat{\mu} := [\mu_1, \mu_3, \mu_5, \ldots, \mu_{2n-1}]^\top$ to denote the vector with entries given by (8). The next assumption is standard.

Assumption 2: For all i the parameters θ_i are positive rational numbers, and $\theta_i \neq \theta_j$, for all $i \neq j$. □

To facilitate our analysis, the ES shall also implement the following dynamics with states $\xi_1 \in \mathbb{R}^n$ and $\xi_2 \in \mathbb{R}^{n\times n}$:

$$\varepsilon_1\dot{\xi}_1 = -\xi_1 + G(\hat{\mu}, u), \ \varepsilon_1\dot{\xi}_2 = -H(\hat{\mu}, u)\xi_2 + G(\hat{\mu}, x), \tag{9}$$

where $\varepsilon_1 > 0$ is a small tunable parameter satisfying $0 < \varepsilon_2 \ll \varepsilon_1$, and where the mappings $G : \mathbb{R}^n \times \mathbb{R}^n \to \mathbb{R}^n$ and $H : \mathbb{R}^n \times \mathbb{R}^n \to \mathbb{R}^{n\times n}$ are given by $G(\hat{\mu}, u) := \frac{2}{a}\hat{\mu}\phi(u)$, $a > 0$, and $H(\hat{\mu}, u)$ has entries satisfying $H_{ij} = H_{ji}$ and

$$H_{ii} = \frac{16}{a^2}\left(\hat{\mu}_i^2 - \frac{1}{2}\right)\phi(u), \ H_{ij} = \frac{4}{a^2}\hat{\mu}_i\hat{\mu}_j\phi(u), \ \forall\ i \neq j.$$

We can simultaneously study different types of ES algorithms by updating the argument of ϕ via the feedback rule

$$u = x + a\hat{\mu}, \tag{10}$$

and by assigning different dynamics to the auxiliary state x. In this paper, we focus on three different types of ES dynamics with persistent jamming of gradient directions modeled by a state $q \in \{-1, 1\}$. Namely:

1) Gradient descent based ES dynamics (GDES) [14], [21]:
$$\dot{x} = F_q(\xi_1) := -kq\xi_1, \quad C = \mathbb{R}^n, \tag{11}$$
2) Newton-Like ES dynamics (NLES) [15], [16]:
$$\dot{x} = F_q(\xi_2) := -kq\xi_2, \quad C = \mathbb{R}^n, \tag{12}$$
3) Hybrid accelerated ES dynamics (HAES) [17]:
$$C = \mathbb{R}^n \times \mathbb{R}^n \times [\delta, \Delta], \ D = \mathbb{R}^n \times \mathbb{R}^n \times \{\Delta\}, \tag{13a}$$
$$\left(x^+, y^+, z^+\right) = G_u(x) := (x, x, \delta), \tag{13b}$$
$$(\dot{x}, \dot{y}, \dot{z}) = F_q(\psi, \xi_1) := \left(\tfrac{2}{z}(y-x), -qzk\xi_1, \tfrac{1}{2}\right) \tag{13c}$$
where $\psi := (x, y, z)^\top$, $\Delta > \delta > 0$ are selected to satisfy the condition $\Delta^2 - \delta^2 \geq 1/(2k\kappa)$, [17, Thm. 2].

Note that the switching signal q turns all the dynamics (11)-(13) into switching/hybrid systems.

C. Main Results

The following theorem corresponds to the first main result of this paper. It characterizes, for each ES algorithm, a family of persistent jamming attacks q under which the controllers *preserve* their ability to solve the ES problem (5). For the GDES and the NLES, we state the stability properties with respect to the set (singleton) $\mathcal{O} := \{u^*\}$, whereas for the HAES we use $\mathcal{O} := \{u^*\} \times \{u^*\} \times [\delta, \Delta]$. We also use the set $\mathcal{T} := [0, N_0] \times [0, T_0] \times Q$ to assert the stability properties of the hybrid automaton (6). The bounds of the theorem are presented in increasing order of complexity.

Theorem 1: Consider the ES dynamics given by (7), (9), and (11)-(13), interconnected with the hybrid automaton (6). Let ϕ be any function satisfying Assumption 1, and let $\eta_1 > 0$. Then, the compact set $\mathcal{A} := \mathcal{T} \times \mathcal{O} \times \{0\} \times \mathbb{T}^n$ is SGPAS as $(\varepsilon_2, a, \varepsilon_1) \to 0^+$ whenever $0 < \eta_2 < 1/(1+\gamma)$, where:

(a) For *NLES*: $\gamma = 1$.
(b) For *GDES*: $\gamma = \ell/\kappa$.
(c) For *HAES*: $\gamma = 24\frac{\max\{1,2k\Delta\delta\ell\}\max\left\{1,2k\Delta_{\max}^2\ell\right\}}{\min\{1,k\Delta\delta\kappa\}\min\{1,2k\delta^2\kappa\}}$. □

In general, the conditions on η_1 and η_2 provided by Theorem 1 are only sufficient. However, in certain cases they are also necessary. In particular, for the GDES and the NLES, the cost function $\phi = u^2$ induces instability when $\eta_2 \geq \eta_2^*$.

Remark 1: For the NLES, the result of Theorem 1 establishes that SGPAS of the minimizer of ϕ is guaranteed whenever the activation time of the jamming signal q is persistently less than 50%. Surprisingly, the bound on η_2 is independent of the Hessian parameters of ϕ. □

Remark 2: For the GDES, Theorem 1 provides an intuitive result: the larger the condition number of ϕ, the less frequent the attacks need to happen in order to guarantee SGPAS. Note that for quadratic positive definite functions of the form $\phi(u) = \frac{1}{2}u^\top Qu + Lu + b$, the condition number γ is given by the ratio $\lambda_{\max}(Q)/\lambda_{\min}(Q)$. Thus, the symmetry of the level sets of ϕ provide qualitative information on how resilient is the ES system to gradient jamming. □

Remark 3: For the HAES, the result of Theorem 1 establishes a bound on η_2 that not only depends on the coefficients (κ, ℓ) of the cost ϕ, and the gain k of the gradient, but also on the tunable parameters (δ, Δ) that characterize the restarting frequency of the momentum state y and the timer z. Note that, whenever the parameters of the controller are selected such that $\ell > \frac{1}{2k\delta\Delta} > \kappa$, the constant γ in Theorem 1 simplifies to $\gamma = (\ell/\kappa)^2\zeta$ with $\zeta := 48\Delta^3/\delta^3$. Since $\gamma \geq 1$, this result uncovers a trade-off between the fast convergence of the HAES and the less conservative bound for η_2 obtained in the GDES. Thus, a jamming signal q that may destabilize the HAES may not necessarily destabilize the GDES. A similar conclusion can be made for the NLES. □

The previous observation suggests that in some cases it might be of interest to continuously switch between GDES and NLES depending on the level of attacks acting on the system. The following theorem addresses this case.

Theorem 2: Consider the ES dynamics given by (7), (9), and (11)-(12), interconnected with the hybrid automaton (6). Let ϕ be any function satisfying Assumption 1. Then, the compact set $\mathcal{A} := \mathcal{T} \times \{u^*\} \times \{0\} \times \mathbb{T}^n$ is SGPAS as $(\varepsilon_2, a, \varepsilon_1) \to 0^+$ whenever $\eta_2 = 0$ and $0 < \eta_1 < \eta_1^*$, where

$$\eta_1^* = \frac{2k\min\{1,\kappa\}}{\ln(\max\{1,\ell^2\}) - \ln(\min\{1,\kappa^2\})}.$$

The result of Theorem 2 establishes a sufficient upper bound on how frequently an ES controller can switch between GDES and NLES in order to preserve the SGPAS property. Note that this result can also be used in contexts where there are no attacks acting on the controller, e.g., when it is of interest to use GDES to bring the trajectories to a neighborhood of u^*, and then use NLES to fine tune the input u. To the best knowledge of the authors, this result is completely new in the context of extremum seeking.

IV. ANALYSIS

Our analysis starts by constructing a unified model that formalizes the "interconnection" described in Theorems 1-2.

A. Unified Modeling Framework

Let $\sigma := (\vartheta, \psi)$, where $\psi = x$ for the GDES and the NLES, and $\psi = (x, y, z)$ for the HAES, and $p = \dim(\psi)$. First, we define a set-valued map F_σ as follows

$$F_\sigma(\sigma, \xi_1, \xi_2) := F_M(\vartheta) \times \{F_q(\psi, \xi_1, \xi_2)\}, \qquad (14)$$

where F_M is given by (6b), and F_q is defined in equations (11)-(13) for each of the ES dynamics. Next, we define the set $C_\sigma := C_M \times C$, where C_M is defined in (6a) and C is defined in equations (11)-(13) for each ES. Subsequently, we define two set-valued mappings $G_{\sigma,1}$, $G_{\sigma,2}$ as follows:

$$G_{\sigma,1}(\sigma) := G_M(\vartheta) \times \{\psi\},\ G_{\sigma,2}(\sigma) := \{\vartheta\} \times \{G_u(\psi)\}, \qquad (15)$$

where $G_u(\psi) = x$ for the GDES and NLES, and G_u is given by (13b) for the HAES. Next, we define two sets $D_{\sigma,1}, D_{\sigma,2}$ as follows: $D_{\sigma,1} := D_M \times \mathbb{R}^p$, and $D_{\sigma,2} := C_M \times D$, where D is given by (13a) for the HAES, and $D := \emptyset$ for the GDES and the NLES. Using this construction, the interconnection of the hybrid automaton (6) and the switching ES dynamics can be modeled by the following HDS with states $(\sigma, \xi_1, \xi_2, \mu)$, flow set given by $C_\sigma \times \mathbb{R}^n \times \mathbb{R}^n \times \mathbb{T}^n$, continuous-time dynamics given by the differential inclusion

$$\begin{pmatrix} \dot{\sigma} \\ \dot{\xi}_1 \\ \dot{\xi}_2 \\ \dot{\mu} \end{pmatrix} \in \begin{pmatrix} F_\sigma(\sigma, \xi_1, \xi_2) \\ \frac{1}{\varepsilon_1}\left(-\xi_1 + G(\hat{\mu}, x + a\hat{\mu})\right) \\ \frac{1}{\varepsilon_1}\left(-H(\hat{\mu}, x + a\hat{\mu})\xi_2 + G(\hat{\mu}, x + a\hat{\mu})\right) \\ \frac{1}{\varepsilon_2}2\pi\mathcal{R}_\theta\mu \end{pmatrix}, \qquad (16)$$

jump set given by $D_\sigma \times \mathbb{R}^n \times \mathbb{R}^n \times \mathbb{T}^n$, and discrete-time dynamics given by the difference inclusion

$$(\sigma^+, \xi_1^+, \xi_2^+, \mu^+) \in G_\sigma(\sigma) \times \{\xi_1\} \times \{\xi_2\} \times \{\mu\}, \qquad (17)$$

where

$$G_\sigma(\sigma) := \begin{cases} G_{\sigma,1}(\sigma), & \text{if } \sigma \in D_{\sigma,1} \\ G_{\sigma,2}(\sigma), & \text{if } \sigma \in D_{\sigma,2} \\ G_{\sigma,1}(\sigma) \cup G_{\sigma,2}(\sigma), & \text{if } \sigma \in D_{\sigma,1} \cap D_{\sigma,2}. \end{cases} \qquad (18)$$

This map captures the jumps of the hybrid automaton (i.e., switches of q) *and* any intrinsic jump of the ES controllers (11)-(13). Naturally, the solutions of this HDS are not unique.

B. Averaging and Singular Perturbation Analysis

The previous HDS is in standard form for the application of singular perturbation theory for hybrid systems [22], with μ acting as fast state in the flows. By using (8), and standard averaging arguments in ES (see [12], [13]), it is easy to compute the average dynamics of the system by averaging the flow map along $t \mapsto (\hat{\mu})$. The resulting average system has states (σ, ξ_1, ξ_2), flow set given by $C_\sigma \times \mathbb{R}^n \times \mathbb{R}^n$, flow map given by

$$\begin{pmatrix} \dot{\sigma} \\ \dot{\xi}_1 \\ \dot{\xi}_2 \end{pmatrix} \in \begin{pmatrix} F_\sigma(\sigma, \xi_1, \xi_2) \\ \frac{1}{\varepsilon_1}\left(-\xi_1 + \nabla\phi(x) + \mathcal{O}(a)\right) \\ \frac{1}{\varepsilon_1}\left(-\nabla^2\phi(x)\xi_2 + \nabla\phi(x) + \mathcal{O}(a)\right) \end{pmatrix}, \tag{19a}$$

jump set given by $D_\sigma \times \mathbb{R}^n \times \mathbb{R}^n$, and a jump map given by

$$\left(\sigma^+, \xi_1^+, \xi_2^+\right) \in G_\sigma(\sigma) \times \{\xi_1\} \times \{\xi_2\}. \tag{20}$$

In turn, this HDS is also in standard form for the application of singular perturbation theory, with the states (ξ_1, ξ_2) modeling the fast dynamics. To analyze this system, we set $\mathcal{O}(a) = 0$, as a structural perturbation, and we compute the reduced hybrid dynamics, which are obtained by substituting ξ_1 and ξ_2 in the right-hand side of $\dot{\sigma}$ by their equilibrium points $\xi_1^* := \nabla\phi(x)$ and $\xi_2^* = \left(\nabla^2\phi(x)^{-1}\right)\nabla\phi(x)$, which are exponentially stable under Assumption 1 (with fixed x). The resulting reduced dynamics are given by

$$\sigma \in C_\sigma, \quad \dot{\sigma} \in F_\sigma(\sigma, \nabla\phi, \nabla^2\phi^{-1}\nabla\phi) \tag{21a}$$
$$\sigma \in D_\sigma, \quad \sigma^+ \in G_\sigma(\sigma). \tag{21b}$$

C. Switching Reduced Average Dynamics

We now study the stability properties of the HDS (21) for each of the ES dynamics. Since the set $\mathcal{T}$ is forward invariant under (6), it suffices to study the convergence of the state ψ. In all cases, we assume that Assumption 1 holds.

Lemma 2: Consider the HDS (21) with F_q given by (11) and $G_u(\psi) = x$. Then, the set $\mathcal{A} = \{u^*\} \times \mathcal{T}$ is UGAS whenever $\eta_1 > 0$ and $0 < \eta_2 < 1/(1+\gamma)$, where γ is defined in item (b) of Theorem 1. □

Proof: Consider the quadratic Lyapunov function $V(x) = \frac{1}{2}|x - u^*|^2$. When $q = 1$, the time derivative of V satisfies

$$\dot{V}(x) = -k(x - u^*)^\top \nabla\phi(x) \le -\kappa k|x - u^*|^2 = -\lambda_s V(x),$$

where $\lambda_s = 2\kappa k$. Similarly, when $q = -1$ we obtain

$$\dot{V}(x) \le k|x - u^*||\nabla\phi(x)| \le k\ell|x - u^*|^2 = \lambda_u V(x),$$

where $\lambda_u = 2\ell k$. Thus, $\frac{\lambda_s}{\lambda_s + \lambda_u} = \frac{1}{1 + \frac{\ell}{\kappa}}$. The result follows by Lemma 6 in the Appendix with $\omega = 1$ and $D = \emptyset$. ■

Lemma 3: Consider the HDS (21) with F_q given by (12) and $G_u(\psi) = x$. Then, the set $\mathcal{A} = \{u^*\} \times \mathcal{T}$ is UGAS whenever $\eta_1 > 0$ and $0 < \eta_2 < 1/(1+\gamma)$, where γ is defined in item (a) of Theorem 1. □

Proof: Consider the Lyapunov function $V(x) = \frac{1}{2}|\nabla\phi(x)|^2$. By Assumption 1, it satisfies $\frac{\kappa^2}{2}|x - u^*|^2 \le \frac{1}{2}|\nabla\phi(x)|^2 \le \frac{\ell^2}{2}|x - u^*|^2$. When $q = 1$, we have:

$$\dot{V}(x) = -k\nabla\phi(x)^\top \nabla^2\phi(x)[\nabla^2\phi(x)]^{-1}\nabla\phi(x) = -\lambda_s V(x),$$

where $\lambda_s = 2k$. Similarly, when $q = -1$, we obtain

$$\dot{V}(\hat{u}) = k|\nabla\phi(x)|^2 = 2kV(x) = \lambda_u V(x), \quad \lambda_u = 2k,$$

Thus, $\frac{\lambda_s}{\lambda_s + \lambda_u} = \frac{1}{2}$, and the result follows by Lemma 6 in the Appendix using $\omega = 1$ and $D = \emptyset$. ■

Lemma 4: Consider the HDS (21) with F_q given by (13c) and G_u given by (13b). Then, the set $\mathcal{A} := \{u^*\} \times \{u^*\} \times [\delta, \Delta] \times \mathcal{T}$ is UGAS whenever $\eta_1 > 0$ and $0 < \eta_2 < 1/(1+\gamma)$, where γ is given by item (d) of Theorem 1. □

Proof: Consider the Lyapunov function presented in [17]: $V(\psi) = \frac{1}{4}|y - x|^2 + \frac{1}{4}|y - u^*|^2 + kz^2(\phi(x) - \phi(u^*))$. It was shown in [17] that under Assumption 1 this function satisfies $\underline{c}|\psi|^2_{\mathcal{A}} \le V(\psi) \le \overline{c}|\psi|^2_{\mathcal{A}}$, with $\underline{c} := 0.25\min\left\{1, 2k\delta^2\kappa\right\}$, and $\overline{c} := 0.75\max\left\{1, 2k\Delta^2\ell\right\}$. When $q = 1$, it was also shown in [17] that the following inequality holds

$$\dot{V}(\psi) \le -\rho|\psi|^2_{\mathcal{A}} \le -\frac{\rho}{\overline{c}}V(\psi) = -\lambda_s V(\psi), \ \forall \psi \in C, \tag{22}$$

with $\rho := 0.5\min\{\frac{1}{\Delta}, 0.25k\delta\kappa\}$ and $\lambda_s = (2/3\Delta)(\min\{1, k\delta\Delta\kappa\})/(\max\left\{1, 2k\Delta^2_{\max}\ell\right\})$. On the other hand, when $q = -1$ the derivative of V satisfies:

$$\dot{V}(\psi) \le \frac{1}{\delta}|y - x|^2 + k\Delta(1.5|y - x||\nabla\phi(x)| \dots$$
$$+ \frac{1}{2}|y - u^*||\nabla\phi(x)| + \frac{\ell}{2}|x - u^*|^2), \quad \forall\ \psi \in C.$$

Since $|y - x| \le |y - u^*| + |u^* - x|$, it follows that

$$\dot{V}(\psi) \le \frac{1}{\delta}|y - x|^2 + 2k\ell\Delta(|y - u^*||x - u^*| + |x - u^*|^2),$$

for all $\psi \in C$, where we used the Lipschitz property of $\nabla\phi$. Define $\eta := \max\left\{\frac{1}{\delta}, 2k\ell\Delta\right\}$. It then follows that $\dot{V}(\psi) \le 2\eta\left(2|y - u^*|^2 + 2|x - u^*|^2\right) = 4\eta|\psi|^2_{\mathcal{A}}$, for all $\psi \in C_u$. By using the quadratic lower bound of V we obtain $\dot{V}(\psi) \le 4\frac{\eta}{\underline{c}}V(\psi) = \lambda_u V(\psi)$, for all $\psi \in C_u$, which implies that

$$\lambda_u = 4\frac{\eta}{\underline{c}} = \frac{16}{\Delta}\frac{\max\{1, 2k\ell\Delta\delta\}}{\min\{1, 2k\kappa\delta^2\}}.$$

On the other hand, it was shown in [17] that during jumps triggered by ψ the Lyapunov function satisfies $V(\psi^+) \le \exp(-\tilde{\gamma})V(\psi) = (1 - \varrho)V(\psi)$, for all $\psi \in D_u$, where $\tilde{\gamma}$ is given by $\tilde{\gamma} := 1 - \frac{\delta^2}{\Delta^2} - \frac{1}{2k\kappa\Delta^2}$, which satisfies $\tilde{\gamma} \in (0, 1)$ whenever $\Delta^2 - \delta^2 > \frac{1}{2k\kappa}$. The result follows by Lemma 6 in the Appendix with $\omega = 1$. ■

Lemmas 2-4 studied the stability properties of system (21) switching between an unstable mode ($q = -1$) and a stable mode ($q = 1$). The following lemma considers the case when the switching occurs between two stable modes (c.f. Theorem 2). In this case, q simply indexes the two vector fields.

Lemma 5: Consider the HDS (21) with functions F_q given by $F_1(x) = -k\nabla\phi(x)$, $F_{-1}(x) = -k(\nabla^2\phi(x))^{-1}\nabla\phi(x)$, and $G_u(\psi) = x$. Then, the set $\mathcal{A} = \{u^*\} \times \mathcal{T}$ is UGAS whenever $\eta_2 = 0$ and $0 < \eta_1 < \eta_1^*$, where η_1^* is given by Theorem 2. □

Proof: We consider the Lyapunov function $V_1(x) = 0.5|x - u^*|^2$ studied in Lemma 2, and the Lyapunov function $V_{-1}(x) = 0.5|\nabla\phi(x)|^2$ studied in Lemma 3. It follows that $\dot{V}_q \leq -\lambda_s V_q(x)$, for all $q \in \{-1, 1\}$, with $\lambda_s = 2k\min\{1, \kappa\}$. Moreover, $V_p(x) \leq \omega V_q(x)$, for all $(p, q) \in \{-1, 1\}^2$, with $\omega = \max\{1, \ell^2\}/\min\{1, \kappa^2\}$. The result follows by Lemma 6 in the Appendix with $\eta_2 = 0$, $D = \emptyset$.

Since Lemmas 2-5 have established UGAS for each of the switching reduced average dynamics (21), the stability results of Theorems 1-2 follow now directly by singular perturbation theory for hybrid dynamical systems [17], [22, Thm. 2], and by structural robustness of hybrid systems to small additive disturbances [11, Thm. 7.21], see [12]. In particular, by [22, Thm. 2], the singularly perturbed hybrid dynamics (19)-(20) with $\mathcal{O}(a) = 0$ render the set $\mathcal{T} \times \mathcal{O} \times \{0\}$ SGPAS as $\varepsilon_1 \to 0^+$. In turn, by [11, Thm. 7.21], the perturbed HDS (19)-(20) with $\mathcal{O}(a) \neq 0$ render the same set SGPAS as $(a, \varepsilon_1) \to 0^+$. Finally, since the dynamic oscillator (7) renders UGAS the set $\mathbb{T}^n$, and the average system (19)-(20) renders the set $\mathcal{T} \times \mathcal{O} \times \{0\}$ SGPAS, it follows by [22, Thm. 2] that the original HDS (16)-(17) renders the set $\mathcal{A}$ SGPAS as $(\varepsilon_2, a, \varepsilon_1) \to 0^+$. This completes the proofs of Theorems 1 and 2.

V. Numerical Examples

In this section, we illustrate our theoretical results via numerical examples. We consider a static map $\phi(u) = 2(u_1 - 5)^2 + 0.5(u_2 - 10)^2$, which satisfies Assumption 1 with $\kappa = 1$ and $\ell = 4$. We implement the GDES, the NLES and the HAES under persistent gradient jamming. To better illustrate the effect of the attacks, we only attack the first component of ξ_1. In Fig. 3 shows the resulting trajectories of the GDES with parameters $k = 0.1$, $\eta_1 = 0.376$, $\eta_2 = 0.25$, $\tau_1(0,0) = \tau_2(0,0) = 0$, $1/\varepsilon_1 = 0.9$, $a = 0.1$, $\varepsilon_2 = 1\times10^{-3}$, and the frequencies were set such that $2\pi\theta_1 = 8.1$ and $2\pi\theta_2 = 4.2$. The inset shows the frequency of the attacks. In this case, stability is preserved. However, as shown in Fig. 4 with black color, when $\eta_2 = 0.55$ (which violates Theorem 1) the ES controllers becomes unstable. This highlights the importance of the activation bound (3). In Fig. 5 we show the trajectories generated by the HAES and the NLES. For the HAES, we used $k = 0.1$, $\eta_1 = 0.376$, $\eta_2 = 0.25$, and $\tau_1(0,0) = \tau_2(0,0) = 0$, $1/\varepsilon_1 = 0.9$, $a = 0.04$, $\varepsilon_2 = 1\times10^{-3}$. For the NLES we used $k = 0.1$, $\eta_1 = 0.376$, $\eta_2 = 0.25$, and $\tau_1(0,0) = \tau_2(0,0) = 0$, $1/\varepsilon_1 = 0.9$, $a = 0.14$, and $\varepsilon_2 = 1\times10^{-3}$. In Fig. 7 we show a system that switches between two stable modes generated by GDES ($q = 1$) and NLES ($q = -1$) with $\eta_1 = 0.8$ and $\tau_1(0,0) = 0$. For GDES, we used $k = 0.2$, $1/\varepsilon_1 = 0.9$, $a = 0.1$, $\varepsilon_2 = 1\times10^{-3}$, $2\pi\theta_1 = 10$, $2\pi\theta_2 = 8$. For NLES, we used $k = 0.2$, $1/\varepsilon_1 = 0.9$, $a = 0.14$, $\varepsilon_2 = 1\times10^{-3}$, $2\pi\theta_1 = 0.9$, $2\pi\theta_2 = 1.26$.

VI. Conclusions

In this letter, we presented the first analysis of averaging-based ES dynamics under persistent jamming on the signals that provide estimations of the gradient. From and adversarial point of view, such type of attacks are appealing given that they require the persistent modification of only one bit in the controller. We showed that in three different ES dynamics these types of attacks do not induce instability provided their activation time satisfies a particular time-ratio constraint that is dependent on the particular ES dynamics under consideration. Our results were also illustrated via numerical examples. Future directions will consider other

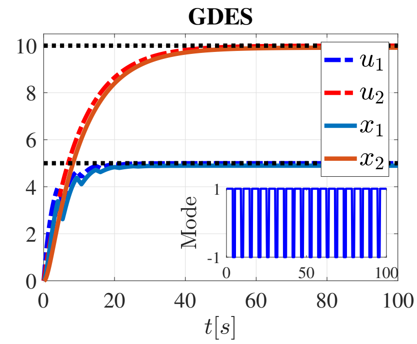

Fig. 3: Evolution in time of GDES under persistent gradient jamming. Since the time-ration constrained is satisfied, the trajectories converge to the solution of (5).

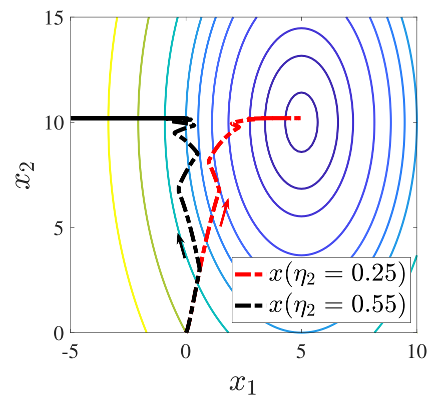

Fig. 4: Comparison between stable and unstable GDES under persistent gradient jamming.

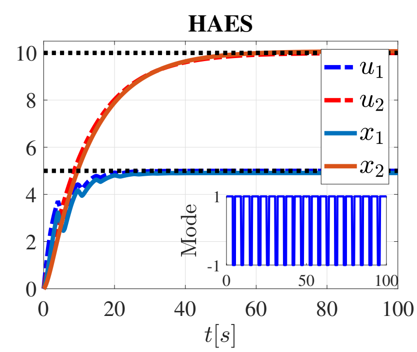

Fig. 5: Evolution in time of HAES under persistent gradient jamming. Since the time-ration constrained is satisfied, the trajectories converge to the solution of (5).

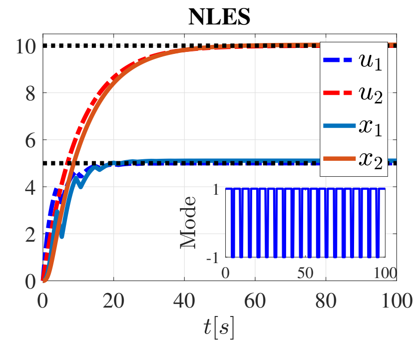

Fig. 6: Evolution in time of NLES under persistent gradient jamming. Since the time-ration constrained is satisfied, the trajectories converge to the solution of (5).

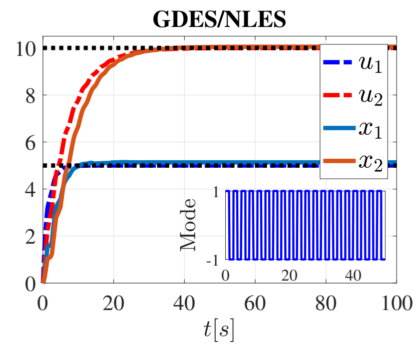

Fig. 7: Switching between GDES and NLES without persistent gradient jamming. Stability is preserved under the dwell-time condition on η_1.

types of attacks, particularly those where the dynamics of the plant play a critical role. Other future directions will study source seeking problems for multi-vehicle systems with jamming attacks of sensors.

APPENDIX

Consider a HDS with state $\upsilon = (\vartheta, (\zeta, s))$, where $\vartheta \in \mathbb{R}^3$, $\zeta \in \mathbb{R}^p$, and $s \in \mathbb{R}$; continuous-time dynamics given by

$$\upsilon \in C_M \times C, \quad \dot{\vartheta} \in F_M(\vartheta), \ \dot{\zeta} = F_q(\zeta, s), \ \dot{s} = \rho, \tag{23}$$

where $\rho > 0$, $F_M : \mathbb{R}^3 \rightrightarrows \mathbb{R}^3$, $C := \mathbb{R}^p \times [\underline{s}, \bar{s}]$ with $\bar{s} > \underline{s} > 0$; discrete-time dynamics given by

$$\upsilon \in D_1 \cup D_2, \qquad \upsilon^+ \in G_{1,2}(\upsilon), \tag{24}$$

where $D_1 := D_M \times C$, $D_2 := C_M \times D$, $D := \mathbb{R}^p \times \{\bar{s}\}$, D_M and C_M are defined in (6), and

$$G_{1,2}(\upsilon) := \begin{cases} G_1(\upsilon), & \text{if } \upsilon \in D_1 \\ G_2(\upsilon), & \text{if } \upsilon \in D_2 \\ G_1(\upsilon) \cup G_2(\upsilon), & \text{if } \upsilon \in D_1 \cap D_2, \end{cases} \tag{25}$$

with set-valued maps $G_1, G_2 : \mathbb{R}^{4+p} \rightrightarrows \mathbb{R}^{4+p}$ defined as

$$G_1(\upsilon) = G_M(\vartheta) \times \{\zeta\} \times \{s\}, \ G_2(\upsilon) = \{\vartheta\} \times \{G(\zeta)\} \times \{\underline{s}\},$$

where $G : \mathbb{R}^p \to \mathbb{R}^p$, and G_M is defined in (6d).

The following lemma is a modest extension of [19, Prop. 2] and [12, Prop. 3] for switched systems with unstable modes where the main state ζ may also experience periodic jumps. In particular, when $D_2 = \emptyset$, the HDS (23)-(24) recovers the models of [19] and [12, Sec. 5]. For completness, the proof can be found in the extended manuscript [].

Lemma 6: Suppose that G and F_q are continuous functions for each $q \in Q := Q_s \cup Q_u \subset \mathbb{Z}_{\geq 1}$, where (Q_s, Q_u) satisfy $Q_s \cap Q_u = \emptyset$. Let $\psi := (\zeta, s)$ and $\mathcal{A} \subset C \cup D$ be compact. Suppose there exist continuously differentiable functions $V_q : (C \cup D) \to \mathbb{R}_{\geq 0}$ such that the following holds:

1) There exists $c_1, c_2 > 0$ such that:
$$e^{c_1}|\psi|^2_{\mathcal{A}} \leq V_q(\psi) \leq e^{c_2}|\psi|^2_{\mathcal{A}}, \ \forall \ (\psi, q) \in (C \cup D) \times Q.$$
2) There exists $\lambda_s > 0$ such that
$$\langle \nabla V_{q_s}(\psi), F_{q_s}(\psi) \rangle \leq -\lambda_s V_{q_s}(\psi), \ \forall \ (\psi, q_s) \in C \times Q_s.$$
3) There exists $\lambda_u > 0$ such that
$$\langle \nabla V_{q_u}(\psi), F_{q_u}(\psi) \rangle \leq \lambda_u V_{q_u}(\psi), \ \forall \ (\psi, q_u) \in C \times Q_u.$$
4) There exists $\omega \geq 1$ such that
$$V_p(\psi) \leq \omega V_q(\psi), \ \forall \ (\psi, q, p) \in (C \cup D) \times Q \times Q.$$
5) There exists $\varrho \in (0, 1) > 0$ such that
$$V_q(\psi^+) - V_q(\psi) \leq -\varrho V_q(\psi), \ \forall \ (\psi, q) \in D \times Q.$$

Then, if $\lambda_s > \eta_1 \ln(\omega) + \eta_2(\lambda_s + \lambda_u)$, the set $\mathcal{A} \times \mathcal{T}$ is UGAS for the HDS (23)-(24). □

Proof: Define $\tau := \ln(\omega)\tau_1 + (\lambda_s + \lambda_u)\tau_2$, and the Lyapunov function $V(\vartheta) = V_q(\psi)e^{\tau}$. Using (6b), it follows that during flows we have $\dot{\tau} \in \ln(\omega)[0, \eta_1] + (\lambda_s + \lambda_u)([0, \eta_2] - \mathbb{I}_{Q_u}(q)) = [0, \gamma] - (\lambda_s + \lambda_u)\mathbb{I}_{Q_u}(q)$, where $\gamma := \eta_2(\lambda_s + \lambda_u) + \eta_1 \ln(\omega)$. It follows that if $q \in Q_s$ and $\psi \in C$, then

$$\begin{aligned} \dot{V}(\vartheta) &\leq V_q(\psi)e^{\tau}\dot{\tau} - \lambda_s V_q(\psi)e^{\tau} \\ &\leq V_q(\psi)e^{\tau}\gamma - \lambda_s V_q(\psi)e^{\tau} \\ &= -(\lambda_s - \gamma)V_q(\psi)e^{\tau} = -\lambda V(\vartheta), \end{aligned} \tag{26}$$

where $\lambda := \lambda_s - \gamma > 0$ whenever $\lambda_s > \eta_2(\lambda_s + \lambda_u) + \eta_1 \ln(\omega)$. Similarly, if $q \in Q_u$ and $\psi \in C$, then

$$\begin{aligned} \dot{V}(\vartheta) &\leq V_q(\psi)e^{\tau}\dot{\tau} - \lambda_s V_q(\psi)e^{\tau} \\ &\leq V_q(\psi)e^{\tau}(\gamma - (\lambda_s + \lambda_u)) + \lambda_u V_q(\psi)e^{\tau} \\ &\leq -(\lambda_s - \gamma)V_q(\psi)e^{\tau} \\ &\leq -\lambda V(\vartheta). \end{aligned}$$

During jumps of the form $\vartheta^+ \in G_2(\vartheta)$, we have that

$$V(\vartheta^+) = V_q(\psi^+)e^{\tau} \leq (1 - \varrho)V_q(\psi)e^{\tau} = (1 - \varrho)V(\vartheta).$$

for all $\upsilon \in D_2$.

Similarly, since $\tau^+ = \tau - \ln(\omega)$, during jumps of the form $\vartheta^+ \in G_1(\vartheta)$, we have

$$\begin{aligned} V(\vartheta^+) = V_{q^+}(\psi)e^{\tau^+} &\leq \max_{q^+ \in Q} V_{q^+}(\psi)e^{\tau}e^{-\ln(\omega)} \\ &\leq \omega V_q(\psi)e^{\tau}e^{-\ln(\omega)} = V(\vartheta). \end{aligned} \tag{27}$$

for all $\upsilon \in D_1$. Combining inequalities (26)-(27), the result follows by [11, Prop. 3.27]. ■

References

[1] S. Amin, A. Cárdenas, and S. Sastry, “Safe and secure networked control systems under denial-of-service attacks,” in *Hybrid Systems: Computation and Control*, vol. 5469, Apr. 2009, pp. 31–45.

[2] J. Giraldo, E. Sarkar, A. A. Cardenas, M. Maniatakos, and M. Kantarcioglu, “Security and privacy in cyber-physical systems: A survey of surveys,” *IEEE Design & Test*, vol. 34, no. 4, pp. 7–17, 2017.

[3] Y. C. Liu, G. Bianchin, and F. Pasqualetti, “Secure trajectory planning against undetectable spoofing attacks,” *Automatica*, vol. 112, pp. 1–10, 2020.

[4] Z. Wu, F. Albalawi, J. Zhang, H. Durand, and P. D. Christofides, “Detecting and handling cyber-attacks in model predictive control of chemical processes,” *Mathematics*, vol. 6, no. 173, pp. 1–22, 2018.

[5] A. Hauswirth, S. Bolognani, G. Hug, and F. Dorfler, “Timescale separation in autonomous optimization,” *IEEE Transactions on Automatic Control*, 2020.

[6] G. Bianchin, J. I. Poveda, and E. Dall’Anese, “Online optimization of switched LTI systems using continuous-time and hybrid accelerated gradient flows,” *arXiv preprint arXiv:2008.03903*, 2020.

[7] U. Premaratne, S. Halgamuge, Y. Tan, and M. Y. Mareels, “Extremum seeking control with sporadic packet transmission for networked control systems,” *IEEE Transactions on Automatic Control*, vol. 7, no. 2, pp. 758–769, 2020.

[8] V. Grushkovskaya, S. Michalowsky, A. Zuyev, M. May, and C. Ebenbauer, “A family of extremum seeking laws for a unicycle model with a moving target: theoretical and experimental studies,” *https://arxiv.org/pdf/1802.09285.pdf*, 2018.

[9] L. Woodward, M. Perrier, and B. Srinivasan, “Real-time optimization using a jamming-free switching logic for gradient projection on active constraints,” *Computers & Chemical Engineering*, vol. 34, no. 11, pp. 1863–1872, 2010.

[10] G. Bianchin, Y. C. Liu, and F. Pasqualetti, “Secure navigation of robots in adversarial environments,” *IEEE Control Systems Letters*, vol. 4, no. 4, pp. 1–6, 2020.

[11] R. Goebel, R. G. Sanfelice, and A. R. Teel, *Hybrid Dynamical Systems*. Princeton, NJ, USA: Princeton University Pressl, 2012.

[12] J. I. Poveda and A. R. Teel, “A framework for a class of hybrid extremum seeking controllers with dynamic inclusions,” *Automatica*, vol. 76, pp. 113–126, 2017.

[13] D. Nešić, Y. Tan, W. H. Moase, and C. Manzie, “A unifying approach to extremum seeking: Adaptive schemes based on estimation of derivatives,” *49th IEEE Conference on Decision and Control*, pp. 4625–4630, 2010.

[14] Y. Tan, D. Nešić, and I. M. Mareels, “On non-local stability properties of extremum seeking control,” *Automatica*, vol. 42, no. 6, pp. 889–903, 2006.

[15] C. Labar, E. Garone, M. Kinnaert, and C. Ebenbauer, “Newton-based extremum seeking: A second-order lie bracket approximation approach,” *Automatica*, vol. 105, pp. 356–367, 2019.

[16] A. Ghaffari, M. Krstić, and D. Nešić, “Multivariable newton-based extremum seeking,” *Automatica*, vol. 48, pp. 1759–1767, 2012.

[17] J. I. Poveda and N. Li, “Robust hybrid zero-order optimization algorithms with acceleration via averaging in time,” *Automatica, provisionally accepted, arXiv:1909.00265*, 2019.

[18] J. P. Hespanha and A. S. Morse, “Stabilization of switched systems with average dwell-time,” *38th IEEE Conference on Decision and Control*, pp. 2655–2660, 1999.

[19] G. Yang and D. Liberzon, “Input-to-state stability for switched systems with unstable subsystems: A hybrid Lyapunov construction,” *53rd IEEE Conf. Decision Control*, pp. 6240–6245, 2014.

[20] A. R. Teel, L. Moreau, and D. Nešić, “A unified framework for input-to-state stability in systems with two time scales,” *IEEE Transactions on Automatic Control*, vol. 48, no. 9, pp. 1526–1544, 2003.

[21] M. Krstic, “Stability of extremum seeking feedback for general nonlinear dynamic agents,” *Automatica*, vol. 36, pp. 595–601, 2000.

[22] W. Wang, A. Teel, and D. Nešić, “Analysis for a class of singularly perturbed hybrid systems via averaging,” *Automatica*, vol. 48, no. 6, pp. 1057–1068, 2012.